

PDF hosted at the Radboud Repository of the Radboud University Nijmegen

The following full text is a preprint version which may differ from the publisher's version.

For additional information about this publication click this link.

<http://hdl.handle.net/2066/75937>

Please be advised that this information was generated on 2018-07-08 and may be subject to change.

Relevance of complete Coulomb interaction matrix for the Kondo problem: Co impurity on Cu(111)

E. Gorelov¹, T. O. Wehling², A. N. Rubtsov³, M. I. Katsnelson⁴, and A. I. Lichtenstein²

¹ *Institut für Festkörperforschung and Institute for Advanced Simulation,
Forschungszentrum Jülich, 52425 Jülich, Germany*

² *I. Institute of Theoretical Physics, University of Hamburg, 20355 Hamburg, Germany*

³ *Department of Physics, Moscow State University, 119992 Moscow, Russia*

⁴ *Institute for Molecules and Materials, Radboud University of Nijmegen, 6525 ED Nijmegen, The Netherlands*

(Dated: May 22, 2009)

The electronic structure of a prototype Kondo system, a cobalt impurity in a copper host is calculated with accurate taking into account of correlation effects on the Co atom. Using the recently developed continuous-time QMC technique, it is possible to describe the Kondo resonance with a complete four-index Coulomb interaction matrix. This opens a way for completely first-principle calculations of the Kondo temperature. We have demonstrated that a standard practice of using a truncated Hubbard Hamiltonian to consider the Kondo physics can be quantitatively inadequate.

PACS numbers: 73.20.-r; 68.37.Ef; 71.27.+a

Introduction

Scanning tunneling microscopy (STM) has become one of the most basic tools for the manipulation of matter at the atomic scale. Although this experimental technique has reached maturity, the detailed theoretical understanding of experimental data is still incomplete and/or contradictory. One of the most famous examples of atomic manipulation is associated with the surface Kondo effect observed when transition metal ions (like Co) are placed on a metallic surface (such as Cu (111))^{1,2}. The surface Kondo effect is the basis for the observation of surprising phenomena like quantum mirages³, and has attracted a lot of attention and interest in the last few years. Early interpretations of these observations were based on the assumption that only surface states of Cu (111) are involved in the scattering of electron waves by the Co adatoms^{4,5,6}. However, later experiments with Co atoms on the Cu (100) surface (that does not have any surface state)⁷, or in Cu (111) but close to atomic surface steps (that affect the surface states)⁸ have indicated that bulk rather than surface states are responsible for the Kondo effect in these situations. The latter can be important for fine tuning of surface electronic structure, with potential applications to nanotechnology. A recent study of CoCu_n clusters on Cu (111) demonstrated this tunability by atomic manipulation and showed that each atom in the vicinity of the magnetic impurity matters for determining the Kondo effect⁹. Moreover, the relevance of the Kondo effect for the electronic structure of metal surfaces themselves was demonstrated by the discovery of a sharp density of states peak on the Cr (001) surface and its possible interpretation as an orbital Kondo resonance^{10,11,12}.

At the same time, when calculating the Kondo temperatures for real electronic structures a mapping onto one-orbital Anderson impurity model¹³ was used. The realistic atomic geometry of Kondo systems plays a crucial

role in complex electronic properties^{9,14} and it is, a priori, not obvious that a one-orbital Anderson impurity approach is sufficient: even the two-orbital Anderson model demonstrates Kondo physics essentially different from the single-orbital one¹⁵. A recent theoretical investigation of Fe impurities in gold and silver showed that the proper Kondo model corresponds to a S=3/2 spin state¹⁶. A realistic, multi-band consideration of correlation effects in specific solids is possible in the framework of the Local Density Approximation + Dynamical Mean-Field Theory (LDA+DMFT) approach (for review, see Ref. 17). However, formally accurate Quantum Monte Carlo (QMC) calculations are always done with taking into account only the diagonal part of Coulomb interaction^{18,19}, even with realistic hybridization functions obtained in the LDA. This approximation is, strictly speaking, uncontrollable. At the same time, approximate schemes working with the complete Coulomb interaction matrix, such as the perturbative scheme²⁰ which is frequently used to calculate electronic structure of transition metals and alloys^{21,22} are not sufficient to reproduce so subtle correlation features like the Kondo effect, properly. As for the exact diagonalization^{10,11} or numerical renormalization group^{11,15,23} methods they are hardly applicable, due to computational problems, for more than two orbitals per impurity.

The recent progress in continuous time QMC scheme (CT-QMC)^{24,25} makes it perspective to treat the complicated Kondo systems²⁶. Here we will apply this method to calculate Kondo temperatures as well as spectral functions for the case of a Co impurity in bulk Cu, in a Cu (111) surface and on top of a Cu (111) surface. In contrast with all previous calculations we will work with an accurate complete Coulomb interaction U -matrix for correlated d orbitals. The latter can be calculated from first principles in a parameter-free way by the GW technique²⁷ so this approach is completely *ab initio*. Moreover, the CT-QMC method allows to work,

without any essential difficulties, even with the rigorous frequency-dependent U -matrix. As the first step, we present calculations for the static U -matrix, but this restriction is purely technical and can be relatively easily removed in the future, with a growth of available computer resources.

I. MULTI-ORBITAL CT-QMC FORMALISM

The multi-orbital impurity problem with a general U -matrix is described by the effective action

$$\begin{aligned} S_{imp} &= S_0 + S_{int} \\ &= -\sum_{ij\sigma} \int_0^\beta \int_0^\beta \mathcal{G}_{ij}^{-1}(\tau - \tau') c_{i\sigma}^\dagger c_{j\sigma} d\tau d\tau' \\ &\quad + \frac{1}{2} \sum_{ijkl\sigma\sigma'} \int_0^\beta U_{ijkl} c_{i\sigma}^\dagger c_{j\sigma'}^\dagger c_{k\sigma'} c_{l\sigma} d\tau \end{aligned} \quad (1)$$

where i, j, k, l are orbital indices, and σ, σ' are spin indices, \mathcal{G}_{ij} is the local non-interacting Green function for correlated orbitals obtained from the Density Functional Theory (DFT) with the help of optimal projection operator to the impurity d-states:

$$\mathcal{G}_{ij}(i\omega_n) = \sum_{n\mathbf{k}} \frac{\langle d_i | \psi_{n\mathbf{k}} \rangle \langle \psi_{n\mathbf{k}} | d_j \rangle}{i\omega_n + \mu - \varepsilon_{n\mathbf{k}}}; \quad (2)$$

here $\varepsilon_{n\mathbf{k}}$ is the energy spectrum and $\psi_{n\mathbf{k}}$ is the corresponding wave function of our system (metal host with magnetic impurity), described by d_i localized orbitals, and U_{ijkl} is the Coulomb interaction matrix element:

$$U_{ijkl} = \langle i_1 j_2 | V_{12}^{ee} | k_2 l_1 \rangle \quad (3)$$

here $i_1 \equiv d_i(\mathbf{r}_1)$ is local orthogonal wave function for correlated orbitals and V_{12}^{ee} is screened spin-independent Coulomb interaction between electrons at the coordinates \mathbf{r}_1 and \mathbf{r}_2 . We used standard quasiatomic LDA+U parametrization of Coulomb matrix for d-electron via effective Slater integrals or average Coulomb parameter U and exchange parameter J as described in Ref.28. We choose the orbital basis related to spherical harmonics to be sure that magnetic orbital quantum numbers in U_{ijkl} matrix are satisfied the following sum rule: $i + j = k + l$. In this case we will get rid of so-called three-site terms like U_{ikkl} with $i \neq l$ which turns out to result in a strong sign problem in QMC calculations with real spherical harmonics.

Following the general CT-QMC scheme²⁴ we expand the partition function around the Gaussian part of our multiorbital action Eq.(1) which gives the fermionic determinant over the non-interacting Green functions with the rank $2n$:

$$\frac{Z}{Z_0} = \sum_n \frac{(-1)^n}{n! 2^n} \sum_{\{ijkl\sigma\sigma'\}} \int_0^\beta d\tau_1 \dots \int_0^\beta d\tau_n U_{i_1 j_1 k_1 l_1} \dots U_{i_n j_n k_n l_n} \det \mathcal{G}^{2n \times 2n} \quad (4)$$

In order to minimize the number of different interaction vertices we group different matrix elements of the multiorbital Coulomb interactions which have a similar structure of fermionic operators. Since the U_{ijkl} matrix elements are spin independent, one should look over all possible combinations of orbital and spin indices, to generate all terms for the interaction in the action Eq.(1). Some combinations can violate the Pauli principle and should be removed. For CT-QMC algorithm it is useful to represent the interaction Hamiltonian in the following form: $U_{ijkl} c_{i\sigma}^\dagger c_{l\sigma} c_{j\sigma'}^\dagger c_{k\sigma'}$.

The interaction terms can be transformed to the desired form, depending on relations between spin and orbital indices:

(i) if $\sigma \neq \sigma'$, we can just commute $c_{l\sigma}$ and $c_{k\sigma'}$ and then $c_{l\sigma}$ and $c_{j\sigma'}^\dagger$. Another combination of indices, that allows the same commutation, is the following: $\sigma = \sigma'$, $i \neq j$ and $k \neq l$ (the latter two are following from the Pauli principle), and also $j \neq l$. These terms we can transform to the following desirable representation:

$$H_{ijkl}^{int1} = U_{ijkl} c_{i\sigma}^\dagger c_{l\sigma} c_{j\sigma'}^\dagger c_{k\sigma'}. \quad (5)$$

(ii) in the case when $\sigma = \sigma'$ and $j = l$ we can commute $c_{k\sigma'}$ and $c_{j\sigma'}^\dagger$, since in this case $i \neq j$ and $k \neq l$ due to the Pauli principle:

$$H_{ijkl}^{int2} = -U_{ijkl} c_{i\sigma}^\dagger c_{k\sigma} c_{j\sigma}^\dagger c_{l\sigma} \quad (6)$$

After generating all this terms it is useful to collect and *symmetrize* all the terms with identical and equivalent (i.e. $U_{ijkl} c_{i\sigma}^\dagger c_{j\sigma} c_{k\sigma'}^\dagger c_{l\sigma'}$ and $U_{klij} c_{k\sigma'}^\dagger c_{l\sigma'} c_{i\sigma}^\dagger c_{j\sigma}$) quantum numbers.

In order to reduce the fermionic sign problem we introduce additional parameters, α , to optimize the splitting of the Gaussian and interaction parts of the action Eq.(1)

$$\begin{aligned}
S_0 &= \sum_{ij\sigma} \int_0^\beta \int_0^\beta \left(-\mathcal{G}_{ij}^{-1}(\tau - \tau') + \frac{1}{2} \sum_{\{kl\sigma'\}} \alpha_{kl}^{\sigma'} (U_{ilkj} + U_{lijk}) \delta_{\tau\tau'} \right) c_{i\sigma}^\dagger c_{j\sigma} d\tau d\tau', \\
S_{int} &= \frac{1}{2} \sum_{\{ijkl\sigma\sigma'\}} \int_0^\beta U_{ijkl} (c_{i\sigma}^\dagger c_{l\sigma} - \alpha_{il}^\sigma) (c_{j\sigma'}^\dagger c_{k\sigma'} - \alpha_{jk}^{\sigma'}) d\tau.
\end{aligned} \tag{7}$$

One can see, that the first item in (7) on Matsubara frequencies corresponds to bare Green's function

$$\mathcal{G}_{ij}^{-1} = (i\omega_n + \mu) \delta_{ij} - \Delta_{ij}(\omega_n) \tag{8}$$

where Δ is the hybridization matrix. The second term is just a constant which we can absorb to the new chemical potential $\tilde{\mu}$. Therefore we can rewrite the bare Green function in the following matrix form:

$$\tilde{\mathcal{G}}^{-1} = (i\omega_n + \tilde{\mu}) \mathbf{1} - \mathbf{\Delta}, \tag{9}$$

The optimal choice of parameters α_{ij}^σ would lead to effective reduction of interaction terms in the action Eq. (7) and therefore minimization of average perturbation order in Eq. (4).

Note that relation between $\tilde{\mathcal{G}}$ and \mathcal{G} can be represented from Eq. (7) in the following spin and orbital matrix form:

$$\tilde{\mathcal{G}}^{-1} = \mathcal{G}^{-1} - \langle \hat{\alpha} \hat{U} \rangle. \tag{10}$$

Here we used the fact that $U_{ilkj} = U_{lijk}$ following from the definition of the Coulomb matrix elements (3).

We also need to minimize the fermionic sign problem which finally leads us to such expression for diagonal alpha parameters

$$\alpha_\sigma^{ii} + \alpha_{\sigma'}^{jj} = \bar{\alpha}, \tag{11}$$

corresponding to the following interaction fields $U_{ijji} n_{i\sigma} n_{j\sigma'}$. The $\bar{\alpha}$ has to be found iteratively in order to get a proper occupation number of correlated electrons. In the case of half-filled one-band Hubbard model $\bar{\alpha} = 1$ leads to the correct chemical potential shift of the $\frac{U}{2}$ and average $\alpha = \frac{1}{2}$ which corresponds to the Hartree-Fock subtraction. For non-diagonal alpha's which correspond to the fields of general form $U_{ijkl} c_{i\sigma}^\dagger c_{l\sigma} c_{j\sigma'}^\dagger c_{k\sigma'}$, where $i \neq l$ and $j \neq k$ we find the following optimal condition:

$$\alpha_\sigma^{ij} + \alpha_{\sigma'}^{kl} = 0 \tag{12}$$

Since we symmetrize the interaction U matrix it is necessary to extend the definition of the $\hat{\alpha}$ matrix to keep all the terms in the interaction part of initial action (the last item in Eq. (7)). It can be done in the following way^{24,34}: for every U_{ijkl} field in 50% of updates we deliver the α parameters as

$\alpha^{il} = \alpha_{diag}$, $\alpha^{jk} = \bar{\alpha} - \alpha_{diag}$, and in another 50% as

$\alpha^{il} = \bar{\alpha} - \alpha_{diag}$, $\alpha^{jk} = \alpha_{diag}$ for the case of $i = l$ and $j = k$. For non-diagonal fields, i.e. $i \neq l$ and $j \neq k$ $\alpha^{il} = \alpha_{nd}$, $\alpha^{jk} = -\alpha_{nd}$, with 50% probability and $\alpha^{il} = -\alpha_{nd}$, $\alpha^{jk} = \alpha_{nd}$ otherwise. It was found that the sign problem is eliminated in the case when $\alpha_{diag} < 0$ and $\bar{\alpha} \geq 1$ for occupancy $n \geq \frac{1}{2}$ per state and $\alpha_{diag} > 0$, $\bar{\alpha} < 1$ otherwise. The optimal choice of $|\alpha_{diag}|$ parameter is few percent of $|\bar{\alpha}|$ to keep minimal average perturbation order. Another problem is a proper choice of non-diagonal α_{nd} parameter. It is easy to see that α_{nd} is proportional to acceptance probability of non-diagonal field in the case where corresponding bare Green function $\mathcal{G}_{jk} = 0$. Since these processes are unphysical, the natural choice is $\alpha_{nd} = 0$. But it leads to division by zero in the updating the inverse Green function matrix²⁴. On the other hand increasing the α_{nd} parameter causes a sign problem. We find a reasonable choice of α_{nd} to be on the order of 10^{-4} . Moreover for some special cases like the atomic limit, where $\mathcal{G}_{mm}(\tau)$ is constant, a small noise should be added to all the α parameters to avoid numerical divergency.

II. RESULTS

The Co-Cu system is treated as five-orbital impurity model representing 3d electronic shell of the cobalt atom hybridized with a bath of a conduction Cu electrons. The bath Green function was obtained using the first-principle density-functional theory within the supercell approach. For Co impurity atoms in the bulk as well as in / on the Cu (111) surface the bath Green functions were obtained using the Vienna-Ab-Initio simulation package (VASP)^{35,36} using the projector augmented wave (PAW) basis sets³⁷. The density functional calculation for cobalt impurity in the bulk was carried out using CoCu₆₃ supercell structure with lattice constant corresponding to pure copper. The surfaces were modelled by supercells of Cu (111) slabs containing 5 Cu layers with 2×2 and 3×4 lateral extension for Co in and on the surface, respectively. The PAW basis naturally provides the projectors $\langle d_i | \psi_{n\mathbf{k}} \rangle$ required in Eq. (2). In using these PAW projectors, directly, we employ here the same representation of localized orbitals as used within the LDA+U-scheme implemented in the VASP-code itself or as discussed in the context of LDA+DMFT in Ref. 38.

For the problem of a single Co impurity in a bulk cop-

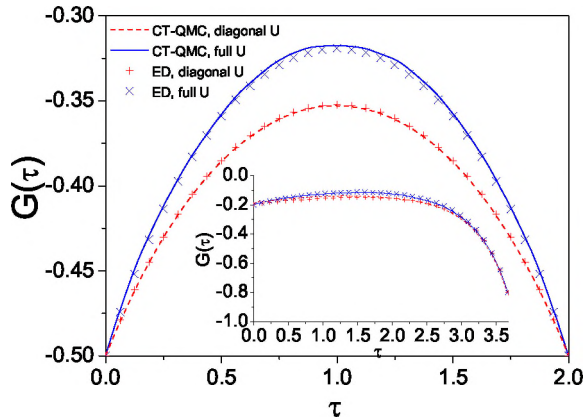


FIG. 1: (color online) Comparison with ED in the atomic limit (without hybridisation to the bath of free electrons). Main graph: $U = 1$ eV, $J = 0.4$ eV $\beta = 2$ eV $^{-1}$, for 5-orbital impurity at half-filling; inset: $U = 2$ eV, $J = 0.7$ eV, $\beta = 3.7$ eV $^{-1}$, for 5-orbital impurity with 8 electrons.

per matrix the basis set of spherical harmonics Y_{lm} is used. In this basis the interaction part of the hamiltonian contains only terms of the following form: diagonal density-density like $H_{int}^{diag} = U_{ijji}n_{i\sigma}n_{j\sigma'}$, where $n_{i\sigma} = c_{i\sigma}^\dagger c_{i\sigma}$ and non-diagonal $H_{int}^{nd} = U_{ijkl}c_{i\sigma}^\dagger c_{j\sigma'}^\dagger c_{k\sigma'} c_{l\sigma}$, where $i \neq j$ and $k \neq l$. The Coulomb matrix for the d -electron shell in the basis of complex harmonics contains 45 non-equivalent diagonal terms. Non-diagonal terms can be further classified to a spin-flips, where $i = l$, $j = k$ and the most general four-orbitals interactions, where this condition is not fulfilled. Notice, that pair-hopping terms ($i = k$, $j = l$) are restricted by symmetry in this basis. In description of d -electron shell we have to involve 20 non-equivalent spin-flips and 64 terms of the most general form.

To find the effects, caused by non-diagonal terms, we used two different interaction Hamiltonian. First, interaction with only diagonal terms was used. In this case there is no sign problem. Then, the complete Coulomb interaction matrix of the $3d$ -electron shell of the cobalt atom with 129 terms was included.

As a benchmark we use impurity problem in the atomic limit, since it can be compared with the result of exact diagonalization (ED) method. The results imaginary time Green function for 5-orbitals model with different chemical potentials corresponding to the d^5 and d^8 configurations are shown in the Fig. 1 in comparison with ED results. The significant difference between density-density (diagonal) interaction and the full vertex can be found both at half-field case with relatively high temperature with the $U = 1$ eV, $J = 0.4$ eV, $\beta = 2$ eV $^{-1}$ and at non-symmetric case even for lower temperature. Note that in the d^8 and d^7 cases the many-body ground-

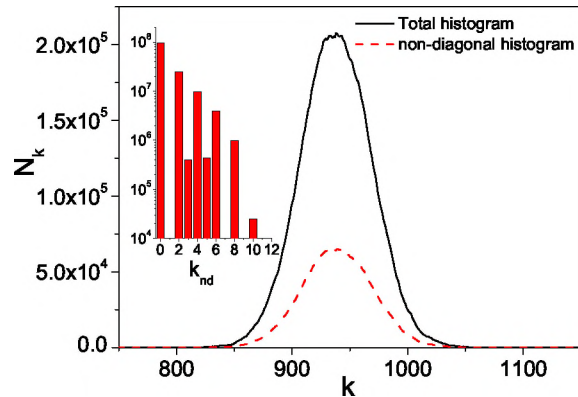


FIG. 2: (color online) Histograms of Monte-Carlo distributions for average perturbation order. Main graph: $U = 4$ eV, $J = 0.7$ eV, $\beta = 10$ eV $^{-1}$ for 5-orbital impurity coupled to realistic Cu-bath with 7 electrons; inset: $U = 4$ eV, $J = 0.7$ eV, $\beta = 1$ eV $^{-1}$ in the case of 5-orbital impurity model, coupled to semi-elliptical bath with bandwidth $W = 0.5$ eV at the half-filling

state have different symmetry for diagonal interactions and non-diagonal full vertex. The results for d^8 configuration with the interaction parameters $U = 2$ eV, $J = 0.7$ eV, $\beta = 3.7$ eV $^{-1}$ are shown in the insert to the Fig. 1. The difference between Green function of the interacting system with full Coulomb interaction and density-density one is visible on the $G(\tau)$. We find a very good agreement between CT-QMC results and ED solution.

In the inset of Fig. 2 we show the distribution of non-diagonal terms, i.e. the contribution of Coulomb fields of the form (5) to the resulting Green function. The zero entry of this histogram counts the number of steps when all the fields contributing to the fermionic determinant (4) were of density-density type. The entry with index 2 show us the number of steps where the average (4) was containing two spin-flip type fields (5). Such situation takes place, for example, when one Coulomb field representing spin-flip $c_{i\uparrow}^\dagger c_{j\downarrow} c_{i\downarrow}^\dagger c_{j\uparrow}$ process was used to construct the determinant.

One can see in the insert of the Fig. 2, that only even orders of interaction histogram have large acceptance probability at high temperature and even the tenth order in non-diagonal interactions has non-zero contribution. The 3-rd and 5-th order contributions exists due to the finite α^{nd} parameter.

Typical distribution of the perturbation order (5-orbital AIM with 7 electrons, $U = 4$ eV, $J = 0.7$ eV, $\beta = 10$ eV $^{-1}$) is shown in Fig. 2, main plot. Dash line denotes the perturbation order during accepted steps that involved non-diagonal fields. The coincidence of distributions maxima of both histograms demonstrate that the

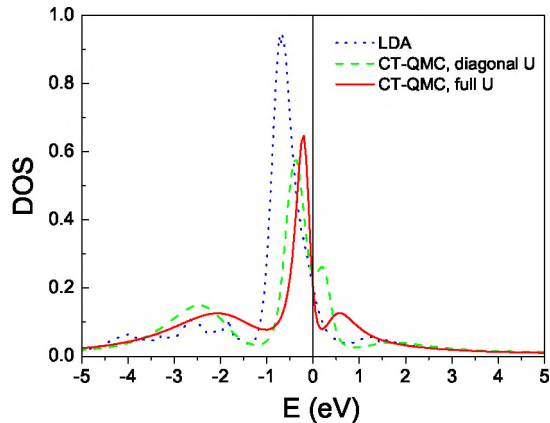


FIG. 3: (color online) Total DOS of 3d orbital of Co atom embedded in Cu matrix. Model parameters: $U = 4$ eV, $J = 0.7$ eV, $\beta = 10$ eV $^{-1}$ for 5-orbital impurity with 7 electrons.

acceptance rate mostly depends on diagonal interactions.

For many-body calculations of the Co impurity in the Cu matrix we need to find the effective d -orbital chemical potential which defines the number of 3d-electrons of cobalt. The particular electronic configuration of a Co atom in a copper matrix is unknown, but the DFT results ($n_d = 7.3$) give us an evidence that it is close to d^7 configuration. Therefore we performed all impurity calculations for cobalt d^7 configuration.

The results of the CT-QMC calculations for $U = 4$ eV and $J = 0.7$ eV are presented in Fig.3 compared to the bare impurity density of states for cobalt impurity in the bulk. There is a pronounced difference between Kondo-like resonance near the Fermi level. In the case of full U -vertex it becomes more narrow and located much closer to the Fermi level. The sign problem for realistic five-band model depends crucially on the symmetry of coulomb vertex U_{ijkl} and magnitude of non-diagonal terms in the bath Green functions \mathcal{G}_{ij} . The most serious problem is related with non-diagonal terms of U -matrix, therefore we use a basis of complex spherical harmonics. In this case there is no so-called three-cite terms or correlated hopping, e.g. U_{ikk} . On the other hand, in this basis, the bath Green-function matrix \mathcal{G}_{ij} for d -electrons has two non-diagonal elements in the bulk of cubic crystals and much more on the surface and in the first layer. Moreover there are lot of small four-site terms U_{ijkl} which result in a large sign problem for surface-atom calculations. The sign problem for a Co impurity in the bulk is not large and average sign is between 0.90 and 0.97 depends on the simulation temperature.

In the case of non-diagonal interaction we used so-called cluster steps which correspond to complex Monte-Carlo updates with more than one additional interaction field. This scheme became essential for spin-flip like interaction or more general U -vertex which can contribute to

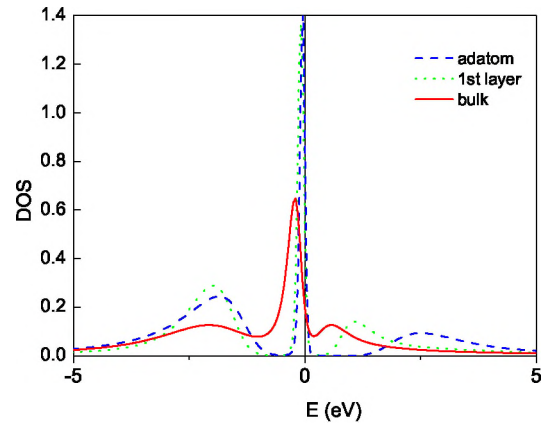


FIG. 4: (color online) Total DOS of 3d orbital of Co atom embedded in the bulk of Cu, into 1-st layer and Co-atom on the Cu(111) surface. Model parameters: $U = 4$ eV, $J = 0.7$ eV, $\beta = 10$ eV $^{-1}$ for 5-orbital impurity with 7 electrons.

the Green-function only in the second or higher order "diagrammatic" expansion and this can let the Monte-Carlo process to explore all the phase space. We note that probability of non-diagonal terms drastically decrease with increasing the hybridization to the bath. Nevertheless, at least for three-band benchmarks we found remarkable effect of the spin-flip terms if the bath Green function has peaks in the vicinity of the Fermi level on the distance of the order of J .

We estimated the renormalization factor $Z = (1 - d\Sigma/dE)^{-1}$ for $U = 4.5$ eV, $J = 0.7$ eV and $\beta = 10$ eV $^{-1}$ and find $Z_{t_{2g}} = 0.5$ and $Z_{e_g} = 0.4$ which shows the reasonable strong interaction of Co d -electrons. We estimate the Kondo temperature (T_K) using the temperature dependence of FWHM for resonance near Fermi level. Since our simulation temperature is very high compared to T_K we can get only order of magnitude of $T_K = 0.1$ eV, which is reasonable for Co-impurity systems.

We also performed the CT-QMC calculation of cobalt impurity on the surface of Cu(111) and embedded into the first copper layer. In contrast to the bulk system the surface one has a large sign problem, related with the relatively large non-diagonal elements of the bath Green functions. Although changing of the sign is a very rare event (less then 0.03% of the accepted steps) and we used a simple constrained sign calculations. Comparison of the different spectral functions for the bulk, surface and first-layer cobalt impurity is presented in Fig. 4. One can see clearly the change of the Kondo resonance width as a function of reduced dimensionality.

CONCLUSIONS

In conclusion, we perform the continuous time QMC calculation of realistic 5-orbital Co impurity in copper and discuss the relevance of non-diagonal part of Coulomb matrix in the Kondo problem. Comparing Figs. 3 and 4 we find that non-density-density terms in the Coulomb vertex are required to obtain quantitative predictions of spectral functions and related properties. The position of the Hubbard peaks and the Kondo peak is markedly changed by spin-flips and other non-diagonal terms of the Coulomb vertex. Thus, obtaining sensitive observables like Kondo temperatures quantitatively requires accounting for these terms. On the other hand hybridization effects like bringing the Co impurity from bulk to the surface and having it on top of the surface can

be quite drastic: As Fig 4 shows, the sharpening of the Kondo resonance and the shifting of the Hubbard bands is much stronger when going from bulk to the surface then on switching on the non-diagonal part of Coulomb matrix. Only the qualitative overall shape the DOS and its response to strong hybridization changes are well described by density-density type terms of the Coulomb vertex.

ACKNOWLEDGEMENTS

The authors acknowledge a financial support from DFG SFB-668 (Germany) RFFI (Russia) and FOM (The Netherlands).

-
- ¹ V. Madhavan, W. Chen, T. Jamneala, M. F. Crommie, and N. S. Wingreen, *Science* **280**, 567 (1998).
- ² J. Li, W.-D. Schneider, and R. Berndt, *Phys. Rev. Lett.* **80**, 2893 (1998).
- ³ H. C. Manoharan, C. P. Lutz, and D. M. Eigler, *Nature* **403**, 512 (2000).
- ⁴ G. A. Fiete and E.J. Heller, *Rev. Mod. Phys.* **75**, 933 (2003).
- ⁵ O. Agam and A. Schiller, *Phys. Rev. Lett.* **86**, 484 (2001).
- ⁶ D. Porras, J. Fernández-Rossier, and C. Tejedor, *Phys. Rev. B* **63**, 155406 (2001).
- ⁷ N. Knorr, M. A. Schneider, L. Diekhöner, P. Wahl, and K. Kern, *Phys. Rev. Lett.* **88**, 096804 (2002).
- ⁸ L. Limot and R. Berndt, *Appl. Surf. Science* **237**, 572 (2004).
- ⁹ N. Néel, J. Kröger, R. Berndt, T. O. Wehling, A. I. Lichtenstein, and M. I. Katsnelson, *Phys. Rev. Lett.* **101**, 266803 (2008).
- ¹⁰ O. Yu. Kolesnichenko, R. de Kort, M. I. Katsnelson, A. I. Lichtenstein, and H. van Kempen, *Nature* **415**, 507 (2002).
- ¹¹ O. Yu. Kolesnichenko, G. M. M. Heijnen, A. K. Zhuravlev, R. de Kort, M. I. Katsnelson, A. I. Lichtenstein, and H. van Kempen, *Phys. Rev. B* **72**, 085456 (2005).
- ¹² T. Hänke, M. Bode, S. Krause, L. Berbil-Bautista, and R. Wiesendanger, *Phys. Rev. B* **72**, 085453 (2005).
- ¹³ Chiung-Yuan Lin, A. H. Castro Neto, and B. A. Jones, *Phys. Rev. Lett.* **97**, 156102 (2006).
- ¹⁴ L. Vitali, R. Ohmann, S. Stepanow, P. Gambardella, K. Tao, R. Huang, V. S. Stepanyuk, P. Bruno, and K. Kern, *Phys. Rev. Lett.* **101**, 216802 (2008).
- ¹⁵ A. K. Zhuravlev, V. Yu. Irkhin, M. I. Katsnelson, and A. I. Lichtenstein, *Phys. Rev. Lett.* **93**, 236403 (2004).
- ¹⁶ T. A. Costi, L. Bergqvist, A. Weichselbaum, J. von Delft, T. Micklitz, A. Rosch, P. Mavropoulos, P. H. Dederichs, F. Mallet, L. Saminadayar, and C. Buerle, *Phys. Rev. Lett.* **102**, 056802 (2009).
- ¹⁷ G. Kotliar, S. Y. Savrasov, K. Haule, V. S. Oudovenko, O. Parcollet, and C. A. Marianetti, *Rev. Mod. Phys.* **78**, 865 (2006).
- ¹⁸ M. I. Katsnelson and A. I. Lichtenstein, *Phys. Rev. B* **61**, 8906 (2000).
- ¹⁹ A. Liebsch and A. Lichtenstein, *Phys. Rev. Lett.* **84**, 1591 (2000).
- ²⁰ M. I. Katsnelson and A. I. Lichtenstein, *Eur. Phys. J. B* **30**, 9 (2002).
- ²¹ J. Minár, L. Chioncel, A. Perlov, H. Ebert, M. I. Katsnelson, and A. I. Lichtenstein, *Phys. Rev. B* **72**, 045125 (2005).
- ²² A. Grechnev, I. Di Marco, M. I. Katsnelson, A. I. Lichtenstein, J. Wills, and O. Eriksson, *Phys. Rev. B* **76**, 035107 (2007).
- ²³ R. Bulla, T. Costi, and T. Pruschke, *Rev. Mod. Phys.* **80**, 395 (2008).
- ²⁴ A. N. Rubtsov, V. V. Savkin, and A. I. Lichtenstein, *Phys. Rev. B* **72**, 035122 (2005).
- ²⁵ P. Werner, A. Comanac, L. de' Medici, M. Troyer and A. J. Millis, *Phys. Rev. Lett.* **97**, 076405 (2006).
- ²⁶ V. V. Savkin, A. N. Rubtsov, M. I. Katsnelson, and A. I. Lichtenstein, *Phys. Rev. Lett.* **94**, 026402 (2005).
- ²⁷ F. Aryasetiawan, M. Imada, A. Georges, G. Kotliar, S. Biermann, and A. I. Lichtenstein, *Phys. Rev. B* **70**, 195104 (2004).
- ²⁸ V. I. Anisimov, F. Aryasetiawan, and A. I. Lichtenstein, *J. Phys.: Condens. Matter* **9**, 767 (1997).
- ²⁹ A. Georges, G. Kotliar, W. Krauth, and M.J. Rozenberg, *Rev. Mod. Phys.* **68**, 13 (1996).
- ³⁰ J. E. Hirsh and R. M. Fye, *Phys. Rev. Lett.* **56**, 2521 (1986).
- ³¹ A. C. Hewson, *The Kondo Problem to Heavy Fermions* (Cambridge Univ. Press, Cambridge, 1993).
- ³² A. I. Lichtenstein, M. I. Katsnelson, and G. Kotliar, *Phys. Rev. Lett.* **87**, 067205 (2001).
- ³³ M. Jarrell and J. E. Gubernatis, *Phys. Rep.* **269**, 133 (1996).
- ³⁴ F. F. Assaad and T. C. Lang, *Phys. Rev. B* **76**, 035116 (2007).
- ³⁵ G. Kresse and J. Hafner, *J. Phys.: Condens. Matter* **6**, 8245 (1994).
- ³⁶ G. Kresse and D. Joubert, *Phys. Rev. B* **59**, 1758 (1999).
- ³⁷ P. E. Blöchl, *Phys. Rev. B* **50**, 17953 (1994).
- ³⁸ B. Amadon, F. Lechermann, A. Georges, F. Jollet, T. O. Wehling, and A. I. Lichtenstein, *Phys. Rev. B* **77**, 205112 (2008).